

Synthesis of nanosized barium titanate/epoxy resin composites and measurement of microwave absorption

M MURUGAN^{*}, V K KOKATE[†], M S BAPAT[#] and A M SAPKAL[†]

Department of E&TC Engineering, Vishwakarma Institute of Information Technology, Pune 411 048, India

[†]Department of E&TC Engineering, College of Engineering, Pune 411 005, India

[#]Department of Allied Sciences, Cummins College of Engineering, Pune 411 052, India

MS received 25 June 2009; revised 24 September 2009

Abstract. Barium titanate/epoxy resin composites have been synthesized and tested for microwave absorption/transmission. Nanocrystalline barium titanate (BaTiO₃ or BT) was synthesized by the hydrothermal method and the composites of BT/epoxy resin were fabricated as thin solid slabs of four different weight ratios. BT was obtained in the cubic phase with an average particle size of 21 nm, deduced from the X-ray diffraction data. The reflection loss (RL) and transmission loss (TL) of the composite materials were measured by the reflection/transmission method using a vector network analyser R&S: ZVA40, in the frequency range 8.0–18.5 GHz (X and Ku-bands). The RL was found to be better than –10 dB over wide frequency bands. The higher RL for lower concentration of BT could be due to increase in impedance matching effects. Low TL values indicate that the absorption by BT is quite low. This could be due to formation of BT in the cubic paraelectric phase.

Keywords. Anechoic chamber; barium titanate; electromagnetic interference and compatibility; epoxy resin composites; microwave absorbers; radio frequency absorbers.

1. Introduction

Absorption of unwanted microwave energy or electromagnetic interference (EMI) is a pressing problem due to the proliferation of complex high speed electronic systems and equipment in the last few decades (Neo and Varadan 2004). Overexposure of microwave energy could be potentially harmful to biological systems and hence, the energy is required to be absorbed. The suitability of a material for use as an EMI shield depends mainly on two factors (Chen *et al* 2004). First, the reflection of microwave energy from the surface of the material should be negligible. This is governed by the impedance matching of the material with that of the free space (377 Ω) and second, the microwave energy should be absorbed within the material (Vinoy and Jha 1995).

For attaining this, composite materials have long been the focus of attention. Here the matrix of the composite is usually a light weight, physically and chemically stable material like foam, epoxy resin and others that do not absorb microwave *per se* but play an important role in determining the overall permittivity and hence the above mentioned impedance matching. A suitable microwave absorbing material like carbon, dielectric material, or magnetic material (Yanfei *et al* 2005) is added to this matrix as lossy filler with a high ability to absorb EMI radiation.

In a recent study (Xiaodong *et al* 2007), barium titanate (BaTiO₃ or BT)/epoxy resin composites, with a particle size of 40–60 nm and tetragonal crystal structure, has been found to be a promising microwave absorbing material. Epoxy resin was selected for the matrix material, because of its thermal stability and its very low dielectric property at microwave frequencies.

The BT is a ferroelectric material for temperature, $T < 120^\circ\text{C}$, when it is in the bulk form. The ferroelectric behaviour is intimately related with the crystal structure. BT exhibits a cubic structure and paraelectric behaviour for $T > 120^\circ\text{C}$. The Ti atom is at the centre of the cube, surrounded by six oxygen atoms forming an octahedron. The barium atoms are at the corners of the cube. When an electric field is applied, the Ti atoms shift from the equilibrium position and thus give rise to an electric dipole moment. For $T < 120^\circ\text{C}$, the structure distorts to a tetragonal one without a centre of symmetry, thus giving rise to a spontaneous moment. BT has, therefore, been widely used as a dielectric and/or piezoelectric material (Jona and Shirane 1962; Moulson and Herbert 1992).

In the quest for increasing microwave absorption, a reduced particle size of BT, i.e. 20 nm, was adopted for the present study (Xiaodong *et al* 2007). Such a size contraction increases the net surface area of BT from 20 m²/g to 47.5 m²/g. This is expected to increase the exposure to microwaves and hence the absorption. Conversely, the

*Author for correspondence (murugan_viit@rediffmail.com)

reduction in the particle size leads to a change in the bulk crystal structure from tetragonal to cubic at room temperature (Zhu *et al* 1997). Analysis of the data indicates that the microwave absorption in our samples could be better than the previously reported value for tetragonal nanoparticles, as is expected for an enhanced surface area.

2. Experimental

2.1 Materials

All the chemicals used were of analytical reagent (AR) grade. The epoxy resin was procured from Shimo Resin Pvt. Ltd. under the trade name SHIMOREZ-400, the density at 25°C being 1.11 g/ml, and the viscosity at 25°C being 12 ± 0.3 Pa.

2.2 Samples

Samples with the following weight ratios of BT to epoxy resin were prepared: (a) BT : epoxy resin 1:10 by weight - BT(1:10),

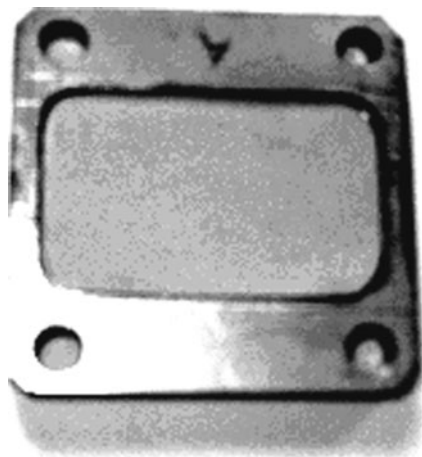


Figure 1. Photograph of WR 90 flange with sample.

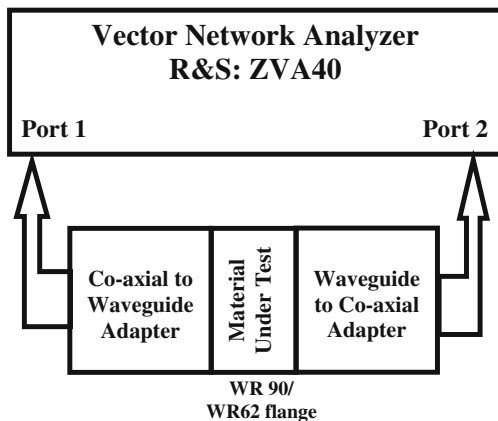


Figure 2. Schematic of the transmission/reflection loss measurement set up.

(b) BT : epoxy resin 1: 5 by weight - BT(1:5), (c) BT : epoxy resin 1: 2 by weight - BT(1:2) and (d) BT : epoxy resin 1: 1 by weight - BT(1:1).

2.3 Method of preparation of BT

Nanocrystalline BT powders were prepared by the hydrothermal method (Andrea *et al* 2005; Yury *et al* 2007; Florentina *et al* 2008; Li *et al* 2009) using cost effective chloride precursor salts (Loba Chemie). The reaction was carried out in an indigenous autoclave at temperatures $<150^\circ\text{C}$ and a corresponding pressure of 75 kg/cm^2 for 3.5 h in the presence of the mineralizer, KOH. The pale yellow product obtained was dried for 24 h in a vacuum oven.

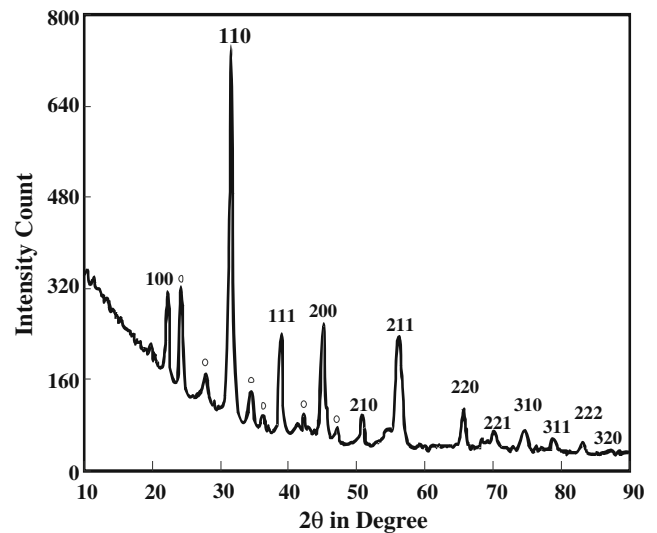


Figure 3. X-ray diffraction pattern of BT/epoxy powder composite BT (1:1).

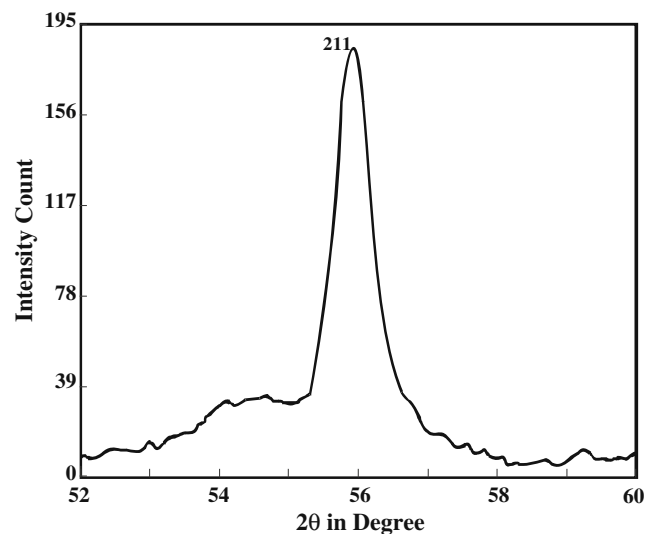


Figure 4. Magnified view of [211] peak in the XRD pattern of BT/epoxy powder composite BT (1:1).

Table 1. Average particle size for BT (1:1).

Index	θ (deg.)	$\cos \theta$	FWHM β (Rad)	Particle size, S (nm)
100	12.1	0.98	5.8×10^{-3}	24.3
110	15.8	0.96	6.7×10^{-3}	21.5
111	19.4	0.94	7.3×10^{-3}	20.2
200	22.5	0.92	8.7×10^{-3}	17.2
210	25.4	0.90	6.9×10^{-3}	21.9
211	28.0	0.88	8.7×10^{-3}	17.9
220	32.8	0.84	11.4×10^{-3}	14.5
310	37.3	0.79	6.9×10^{-3}	24.9
Average particle size				20.6

2.4 Preparation of composite slabs

The epoxy resins were loaded (Athawale *et al* 2008) by adding four different concentrations of BT. For this, the reaction mixtures were prepared by mixing appropriate

quantities of BT, and epoxy resin monomer and hardener in a beaker and heating on a hot plate at 80°C with continuous stirring for 30 min to obtain a paste. On cooling, the homogeneous mixture was cast into rectangular slabs with dimensions 34×22 mm and with a thickness of 1 mm.

2.5 Analysis

X-ray powder diffraction of the composite was obtained using a Philips make PAnalytical XRD machine. Transmission electron microscopy (TEM) images were obtained using the Philips CM-200 instrument at an accelerating voltage of 200 kV. The scanning electron microscopy (SEM) images were obtained on a JEOL-JSM-6360A analytical scanning station. The composites being insulating, were coated with a thin layer of gold to avoid accumulation of charge on the sample during imaging.

3. Measurements

The performance characteristics of the composites were studied by the transmission/reflection method (Afsar *et al* 1986; Behari *et al* 2003) using a vector network analyser R&S: ZVA40, in the X-band and Ku-band frequency range of 8–18.5 GHz. The transmission and reflection losses of

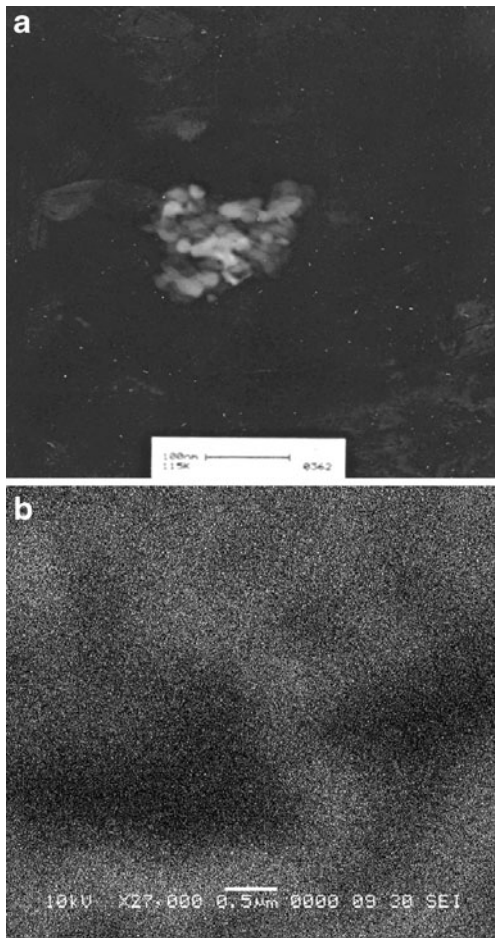


Figure 5. a. TEM of composite of BT/epoxy BT(1:1) and b. SEM of composite of BT/epoxy BT (1:1).

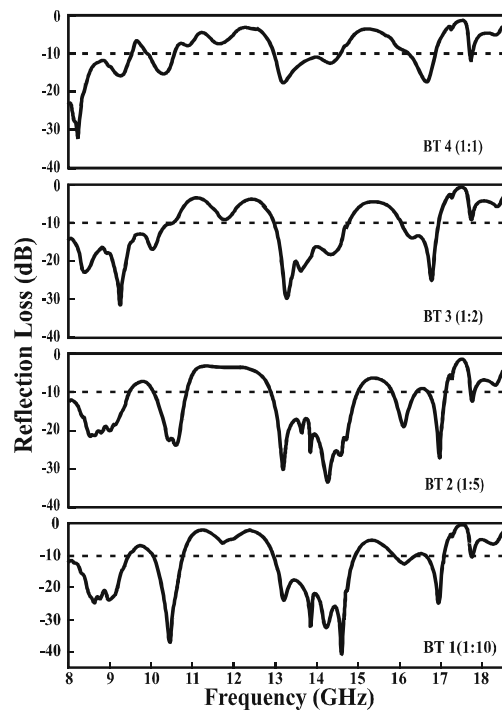


Figure 6. Reflection loss of the composite samples.

Table 2. Summary of results.

Parameters	X-band				Ku-band			
	BT (1:10)	BT (1:5)	BT (1:2)	BT (1:1)	BT (1:10)	BT (1:5)	BT (1:2)	BT (1:1)
Frequency range in GHz with reflection loss of -10 dB or less	8.0–9.5 & 10.0–10.8	8.0–9.5 & 10.0–10.8	8.0–10.3	8.0–9.5 & 9.9–10.6	12.9–14.3 & 15.6–16.9	12.9–14.8, 15.4–15.8 & 16.8–17.1	13.0–14.8 & 16.0–17.0	13.0–14.6 & 16.2–16.9
Bandwidth (GHz)	2.3	2.3	2.3	2.2	2.7	2.6	2.8	2.3
Min. RL (dB)	-39.2	-24.1	-30.1	-31.7	-40.4	-32.6	-29.4	-17.8
Frequency (GHz) of minimum, RL	10.5	10.6	9.3	8.2	14.6	14.3	13.3	13.2

the samples, S_{21} ($= S_{12}$ and S_{11} ($= S_{22}$), respectively were measured by the waveguide method by placing the sample or material under test into the WR 90/WR 62 waveguide flanges, with necessary care while coupling the co-axial to waveguide adapters with the waveguide flange.

Figure 1 shows the flange holding the sample. The configuration of the set up for measuring the S -parameters is as shown in figure 2. Prior to carrying out the actual measurements on the sample, the vector network analyser was calibrated with an open circuit, a short circuit, and the matched load as per the prescribed procedure for R&S: ZVA40.

The performance characteristics of the materials were recorded on the basis of the reflection from the material and transmission through the material. The testing frequency bands were chosen from 8–12.5 GHz (X-band) and 12.5–18.5 GHz (Ku-band) frequency ranges.

4. Results and discussion

Figure 3 shows the XRD (Batllo *et al* 1994) of the composite BT/epoxy resin with 1:1 ratio. The indexed peaks in the XRD pattern correspond to the cubic phase of BaTiO₃. The absence of splitting of 211 peak (figure 4) confirms the cubic phase of BT. The lattice constant is $a = 4.02 \text{ \AA}$. The peaks marked with circles in figure 3 correspond to the presence of BaCO₃ (<10%) that usually results as a consequence of the high pH that is maintained with the help of the mineralizer during the hydrothermal reaction (Joocho *et al* 2003).

The large background, especially at lower angles is due to the epoxy resin matrix. The observation of the cubic phase for the nanoparticles, as opposed to the tetragonal structure for the bulk material at room temperature, is not surprising. In a nanoparticle, the surface energy becomes comparable to the volume energy due to the large surface to volume ratio. This gives rise to an effect akin to surface tension.

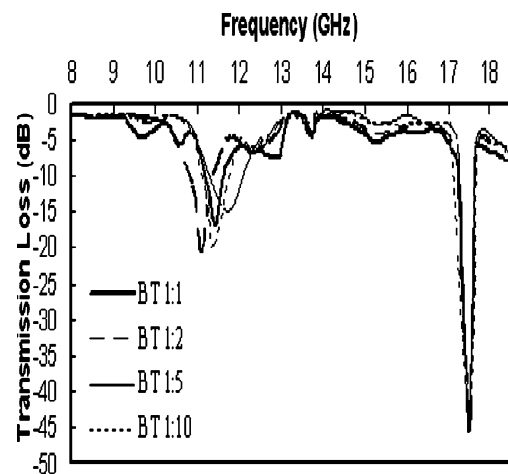
The extent of broadening in BT peaks of the XRD is described by (β), the full width at half maximum (FWHM)

intensity of the peak. The size of the nanoparticles (S) was calculated by the Scherrer's equation (Tae and Yeong 2003),

$$S = \frac{0.9\lambda}{\beta \cos \theta}, \quad (1)$$

where λ is the wavelength ($= 1.5406 \text{ \AA}$), θ the diffraction angle of the given peak, and β the full width at half maximum (FWHM) of the peak. The instrumental contribution of 0.05° has been taken care of by using silicon as a standard and has been subtracted in the calculation of particle size. The particle size calculated for individual peaks is shown in table 1. The average particle size is $\sim 21 \text{ nm}$.

The TEM picture (figure 5(a)) shows that the BT nanoparticles are spherical crystallites of about 20 nm size clustered together in aggregates. The tendency of the nanoparticle to agglomerate and subsequently coalesce into larger particles happens due to the lowering of free energy associated with the surface term on forming larger particles (Sun *et al* 2007). In the present study, though the particles aggregate, they do not form larger particles as the particles are capped. The SEM picture (figure 5(b)) shows that the BT nanoparticles are almost uniformly distributed in the

**Figure 7.** Transmission loss of the composite samples.

entire epoxy resin matrix. There are no signs of major clumping of the particles.

The reflection characteristics vs frequency for all four samples, viz. BT (1:10) through BT (1:1) are as shown in figure 6. As the epoxy resin is presumed to be transparent to electromagnetic waves, the two port calibrations have been carried out by inserting a blank epoxy (with no BT) into the waveguide. Therefore, the performance shown in figure 6 corresponds to the BT powder.

The maximum reflection losses in the X-band for samples BT(1:10) through BT(1:1) are -39.2 dB at 10.5 GHz, -24.1 dB at 10.6 GHz, -30.1 dB at 9.3 GHz and -31.7 dB at 8.2 GHz, respectively. In the case of Ku-band, these values have been noted as -40.4 dB at 14.6 GHz, -32.6 dB at 14.3 GHz, -29.4 dB at 13.3 GHz and -17.8 dB at 13.2 GHz, respectively. The reflection loss of BT (1:10) exhibits better performance as compared to other samples. Its reflection loss is below -10 dB in the frequency range of 8.9 – 9.5 GHz and 10.0 – 10.8 GHz with a total bandwidth of 2.3 GHz in the X-band, whereas its performance in the Ku-band is below -10 dB in the frequency range 12.9 – 14.3 GHz and 15.6 – 16.9 GHz with a total bandwidth of 2.6 GHz and a maximum reflection loss of -40.4 dB was noted at 14.6 GHz. The details are given in table 2.

This result of better reflection loss for a lower concentration of BT, *prima facie* seems to be counter-intuitive. However, it can be explained as follows. In the present study, the measurements of S_{11} and S_{21} have been carried out using the reflection/loss method. Therefore, the reflection loss is solely governed by the impedance mismatch between the free space and the sample. The larger reflection loss for the BT (1:10) sample thus indicates a better matching of impedance.

A careful study of transmission loss (figure 7) along with the reflection loss characteristics helps us in understanding the absorption behaviour of the samples and hence their utility for use in an anechoic chamber. The TL is large at frequencies around 11.5 GHz and 17.5 GHz. Correspondingly, the RL is small around these frequencies indicating high reflectivity. Apart from these two frequencies, the TL characteristic is rather flat and is almost the same for all the BT samples. This indicates that the absorption of the microwaves has saturated for a concentration as low as 1:10 by weight. This is probably due to the large surface area (see § 2) provided by the nanoparticles for microwave absorption. As mentioned above, the TL characteristic is rather flat and the TL loss is never < -1.67 dB.

The amount of power absorbed in the BT samples can be calculated using the basic relation: $P_i = P_r + P_t + P_a$, where P_i , P_r , P_t and P_a are the incident, reflected, transmitted, and absorbed powers, respectively. For example, at around 9 GHz, $P_a/P_i = 0.3$ (i.e. 30% of the incident power is absorbed in 1 mm of BT (1:10)). In a typical anechoic chamber like situation the absorbing layer (the BT samples in our case) is

backed by a conducting plate. If we assume the conducting plate to be purely reflecting, then the microwave would travel through 2 mm of the BT sample and come out on the same side as the incident beam. As the microwave power decreases exponentially due to absorption, the effective RL will be $(0.30)^2 = 0.09$. This corresponds to a value of RL better than -10 dB. This strongly suggests that the material will be suitable for an anechoic chamber in the X and Ku bands, except for frequencies around 11.5 GHz and 17.5 GHz.

5. Conclusions

The important results of our study can be summarized as follows:

- (I) BT powder with a nanoparticle size of 21 nm has been hydrothermally synthesized resulting in the cubic phase.
- (II) Microwave absorption seems to be strong in the X and Ku bands due to increased effective surface area of the nanoparticles, except for frequencies around 11.5 GHz and 17.5 GHz.
- (III) Light weight BT/epoxy resin composites with BT concentrations as low as 1:10 could probably be used in anechoic chambers for the above frequency ranges.
- (IV) In future studies, actual trials on large metal backed samples by the free space method need to be carried out.
- (V) Studies on strontium titanate and calcium titanate are underway to explore the possibility of improving the frequency ranges around 11.5 GHz and 17.5 GHz.

Acknowledgements

The authors would like to thank Prof. C S Garde, Physics Department, V.I.I.T., Pune for his technical inputs and overall guidelines, Dr Raj Kumar, DIAT, Pune, for his support in the measurements and Dr Mohamed Alhousami for the help in making samples. One of the authors (MM) acknowledges BCUD, University of Pune, for financial support. Special thanks to Dr A A Athawale, Department of Chemistry, University of Pune, and Dr Sudha Srivastava, TIFR, Mumbai, for their all round support.

References

- Afsar M U *et al* 1986 *Proc. IEEE* **74** 183
 Andrea T *et al* 2005 *Chem. Mater.* **17** 5346
 Athawale A A *et al* 2008 *J. Rein. Plas. and Compos.* **27** 605

- Batllo F et al 1994 *Proc. of the Ninth IEEE int. symp. on applications of ferroelectrics (ISAF '94)* (Pennsylvania, USA: IEEE) p. 87
- Behari J (ed.) 2003 *Microwave measurement techniques and applications* (New Delhi: Anamaya Pub.) pp. 11–42
- Chen L F, Ong C K, Neo C P and Varadan V V 2004 *Microwave electronics: Measurement and material characterization* (London: John Wiley) pp. 175–205
- Florentina M et al 2008 *Cryst. Growth Des.* **8** 3309
- Jona F and Shirane G 1962 *Ferroelectric crystals* (London: Pergamon) p. 115
- Jooho Moon et al 2003 *J. Eur. Ceram. Soc.* **23** 2153
- Li Y et al 2009 *J. Phys. Chem.* **C113** 4386
- Moulson A J and Herbert J M 1992 *Electroceramics* (London: Chapman and Hall) p. 69
- Neo C P and Varadan V K 2004 *IEEE Trans. Electromagn. Compat.* **46** 102
- Sun W et al 2007 *Chem. Mater.* **19** 1772
- Tae Y K and Yeong D H 2003 *IEEE Trans. Magn.* **39** 3109
- Vinoy K J and Jha R M 1995 *Sadhana* **20** 815
- Xiaodong C et al 2007 *J. Phys. D: Appl. Phys.* **40** 1827
- Yanfei H et al 2005 *J. Appl. Phys.* **98** 084903-1
- Yury V et al 2007 *J. Phys. Chem.* **C111** 7306
- Zhu W et al 1997 *J. Mater. Sci.* **32** 4303